

# Scaling laws for the two-dimensional eight-state Potts model with fixed boundary conditions

M. Baig

*Grup de Física Teòrica & IFAE, Facultat de Ciències, Edifici Cn, Universitat Autònoma de Barcelona, 08193 Bellaterra (Barcelona), Spain*

R. Villanova

*Matemàtica Aplicada, DEE, Universitat Pompeu Fabra, 08028 Barcelona, Spain*

(Received 30 July 2001; published 19 February 2002)

We study the effects of frozen boundaries in a Monte Carlo simulation near a first-order phase transition. Recent theoretical analysis of the dynamics of first-order phase transitions has enabled us to state the scaling laws governing the critical regime of the transition. We check these new scaling laws performing a Monte Carlo simulation of the two-dimensional, eight-state spin Potts model. In particular, our results support a pseudocritical  $\beta(L)$  finite-size scaling of the form  $\beta(\infty) + a_1/L + a_2/L^2$ , instead of  $\beta(\infty) + \theta_1/L^d + \theta_2/L^{2d}$ . Moreover, we obtain a latent heat  $\Lambda_{\text{FBC}} = 0.294(11)$ , which does not coincide with the latent heat analytically derived for the same model if periodic boundary conditions are assumed,  $\Lambda_{\text{PBC}} = 0.486358\dots$

DOI: 10.1103/PhysRevB.65.094428

PACS number(s): 75.10.Hk, 05.10.-a, 05.50.+q, 05.70.Fh

## I. INTRODUCTION

The introduction of computer simulation methods has been a breakthrough in the study of phase transitions in lattice models. The rapid increase in computer power has enabled us to analyze with great accuracy the scaling laws, governed by the critical exponents, and even the corrections to these scaling laws. In such an analysis, finite-size effects must be taken into account carefully.<sup>1</sup> One of these effects, the disturbance from the boundary, has usually been dismissed by the adoption of periodic boundary conditions (PBC's). Nevertheless, in some situations the adoption of periodic lattices may not be adequate, either for practical or theoretical reasons. This is the case of the free boundary conditions used in the analysis of free surfaces or the so-called boundary fields used in the analysis of wetting phenomena. In the present paper we will focus on a particular election of the boundary conditions, the so-called fixed boundary conditions (FBC's), which have been recently applied to spin models<sup>2,3</sup> and gauge models.<sup>4</sup>

Second-order phase transitions exhibit universality. For this reason, all the details of the system near the phase transition point become irrelevant for the critical exponents. By contrast, first-order phase transitions are not universal and, hence, all details of a simulation must be considered carefully. This includes, in particular, the choice of boundary conditions. What are the appropriate set of scaling laws for a first-order phase transition with FBC's? This is the question we address in this paper. Starting from the theoretical analysis of Borgs and Kotecky<sup>5,6</sup> and the work of Medved<sup>7</sup> on the dynamics of first-order transitions, we present the finite-size scaling laws applicable to the case of FBC's and we check them performing a numerical simulation of the two-dimensional (2D) eight-state spin Potts model<sup>8</sup> with FBC's.

The paper is divided as follows. In Sec. II a brief summary of some recent simulations where FBC's have been adopted serves as motivation for a detailed analysis of the finite-size scaling laws which are also presented and discussed. Section III is devoted to a discussion of our numeri-

cal simulation and the results that we have obtained. In Sec. IV we analyze our results in the light of the scaling laws presented in Sec. II. Finally, in Sec. V we give some concluding remarks.

## II. FIXED BOUNDARY CONDITIONS

### A. Motivation for FBC's

Recently, so-called *gonihedric spin models* have been proposed as a laboratory to study discrete versions of string theories.<sup>9</sup> All these simulations have been performed imposing standard periodic boundary conditions on a three-dimensional lattice. Nevertheless, in some cases three intersecting inner planes of spins were fixed to break the large energy degeneracy of the Hamiltonian.<sup>2,3</sup> Due to the periodicity of the boundaries, this is equivalent to fixing the spins belonging to the six planes of the 2D boundary of the 3D cube formed by the spins. Since for a certain range of the coupling parameter, in particular for  $\kappa=0$ , the transition is clearly of first order, the analysis of the finite-size effects should have been done using the scaling laws presented in this paper. We expect that the application of the FBC scaling laws may overcome some anomalies recently observed in the analysis of this transition.<sup>10</sup>

Another situation where knowledge of the FBC scaling laws seems to be crucial is the issue of the triviality of lattice QED. Indeed, it has been claimed that the formation of artificial monopole structures, which close over the boundaries, in a simulation of the 4D U(1) gauge model may be responsible for turning the phase transition of this model from second to first order.<sup>11</sup> To avoid this problem, originated probably by an incorrect choice of the boundaries, it was suggested to perform Monte Carlo simulations on a lattice with the topology of a sphere. Along these lines, Baig and Fort<sup>4</sup> proposed the adoption of FBC's to simulate a spherical topology. Effectively, to fix all variables belonging to the 3D border to unity is the higher-dimensional equivalent of converting a 2D plane square lattice to the 2D surface of a sphere by collapsing the lines of the border to a single point.

Nevertheless, to discriminate between a first- or second-order nature for a transition, an accurate analysis of the data produced is necessary, and, in particular, this will be only possible if one knows for certain the applicable scaling laws.

### B. Scaling laws

Although speaking properly no critical exponents can be defined for first-order phase transitions, it is usual to define a set of characteristic exponents, together with a set of scaling laws borrowed from those of second-order phase transitions. The pioneering work of Privman and Fisher,<sup>12</sup> Binder and Landau,<sup>13</sup> and Challa *et al.*,<sup>14</sup> provided a phenomenological understanding of the scaling for first-order transitions. A more rigorous theoretical justification for these first-order scaling laws was presented by Borgs and Kotecky.<sup>5,15</sup> The formulation of its applicability to finite-size scaling expressions in terms of the lattice size was the work of Borgs, Kotecky and Miracle-Solé<sup>16</sup> and, independently, of Janke.<sup>17</sup> But in all these developments the existence of periodic boundary conditions was assumed. Recently, though, Borgs and Kotecky<sup>6</sup> have extended their analysis to include surface effects in addition to the standard volume effects which govern first order transitions. Following this work, Medved'<sup>7</sup> has deduced the scaling laws for the spin Potts model in the presence of surface effects, in particular adopting boundary conditions other than the periodic ones.

Following the general analysis of Medved',<sup>7</sup> finite-size scaling laws in terms of the lattice size for the case of fixed boundary conditions can easily be deduced. They are summarized in Table I, together with the standard laws for periodic conditions. In the rest of this paper we will check these modified scaling laws with the results of our numerical simulation.

It should be noticed that the suggestion that in the case of free boundary conditions every transition is shifted by a  $1/L$  correction term caused by surface effects is quite old. Binder,<sup>18</sup> for instance, reports on a series of experimental results<sup>19</sup> supporting this conclusion.

TABLE I. Scaling laws for periodic and fixed boundary conditions.

PBC	FBC
$\beta_c^{peaks}(L) = \beta_c(\infty) + \frac{\theta_1}{L^d} + O\left(\frac{1}{L^{2d}}\right)$	$\beta_c(\infty) + \frac{a_1}{L} + O\left(\frac{1}{L^2}\right)$
$C_{max}(L) = \gamma_0 + \gamma_2 L^d + O\left(\frac{1}{L^d}\right)$	$c_0 + c_2 L^d + O(L^{d-1})$
$\chi_{max}(L) = \delta_0 + \delta_2 L^d + O\left(\frac{1}{L^d}\right)$	$e_0 + e_2 L^d + O(L^{d-1})$
$B_{min}(L) = \Phi_0 + \frac{\Phi_1}{L^d} + O\left(\frac{1}{L^{2d}}\right)$	$B_0 + \frac{B_1}{L} + O\left(\frac{1}{L^2}\right)$

### III. NUMERICAL SIMULATION

To test the scaling laws of Table I, we have performed a numerical simulation of the 2D eight-state spin Potts model defined by the partition function

$$Z_{potts} = \sum_{\{\sigma_i\}} e^{-\beta E}, \quad (1)$$

where the energy is

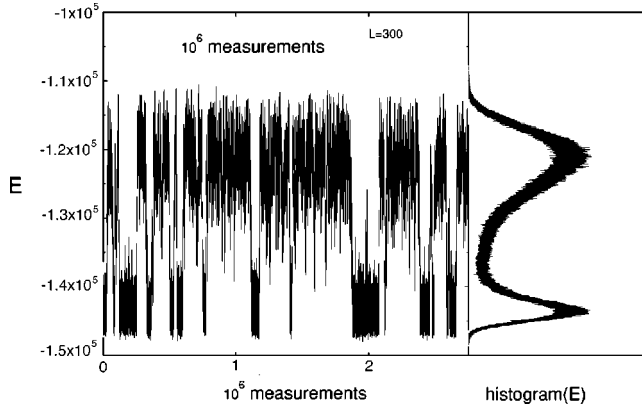
$$E = - \sum_{\langle ij \rangle} \delta_{\sigma_i \sigma_j} \quad (\sigma_i = 1, \dots, 8), \quad (2)$$

with  $\beta = J/kT$  in natural units. It is well known that this model exhibits a first-order phase transition<sup>20</sup> and for this reason it has been chosen as a test model in several previous studies.

Fixed boundary conditions have been implemented along the lines stated by Baig and Fort.<sup>4</sup> In a 2D grid with points labeled by  $(n_x, n_y)$ , all spins corresponding to the lattice points  $(1, n_y)$  and  $(n_x, 1)$  for  $n_x, n_y = 1, \dots, L$  have been fixed during the entire simulation at its initial values  $\sigma = 1$ .

TABLE II. Monte Carlo parameters of the simulation.  $L^2$  is the lattice size,  $n_{\text{therm}}$  the number of Monte Carlo sweeps during thermalization, and  $n_{\text{prod}}$  the number of production runs. Measurements were taken every  $n_{\text{flip}} = 8$  Monte Carlo sweeps for all the simulations.

$L$	$\beta_{MC}$	$n_{\text{therm}}$	$n_{\text{prod}}$	$\tau_e$	$\tau_e^{\text{int}}$	$\frac{n_{\text{therm}}/n_{\text{flip}}}{\tau_e}$	$\frac{n_{\text{prod}}/n_{\text{flip}}}{2 \tau_e}$
70	1.3343	100 000	6 000 000	144	128(12)	87	2604
84	1.3363	100 000	6 000 000	208	240(25)	60	1803
100	1.3378	150 000	8 000 000	357	394(38)	53	1441
126	1.33909	250 000	8 000 000	883	847(122)	35	567
150	1.3398	400 000	10 000 000	1320	1341(215)	38	474
200	1.3407	900 000	12 000 000	4664	5434(1582)	24	161
226	1.34102	1 200 000	16 000 000	7287	6991(1476)	21	138
250	1.341205	1 600 000	18 000 000	9072	9700(2454)	22	124
278	1.34138	2 200 000	18 800 000	11743	16969(5058)	23	100
300	1.34146	3 000 000	22 000 000	15429	27765(12969)	24	89
350	1.34162	4 000 000	32 700 000	25632	53623(29055)	20	80

FIG. 1. Energy time series for  $L=300$  and  $\beta_{MC}=1.34146$ .

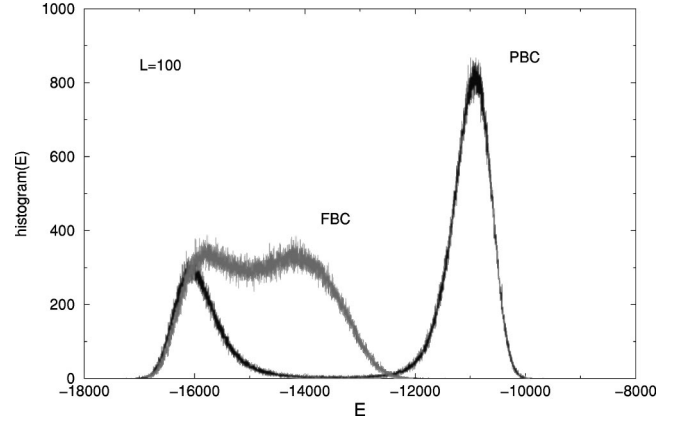
With this precaution, the structure of the program, which implements PBC's, assures the persistence of the frozen boundary.

We have performed the lattice updating applying a well-tested heat bath algorithm. During the simulation we recorded time series files for the energy  $E$  and the magnetization  $M$  defined as

$$M = \frac{q \max\{n_i\} - L^d}{q-1}, \quad (3)$$

where  $q=8$  and  $n_i$  is the number of spins in a given orientation.

Table II summarizes the details of the simulations that have been performed from  $L=70$  up to  $L=350$ . The number of production Monte Carlo sweeps varies from  $n_{\text{prod}}=6\,000\,000$  for  $L=70$ , to  $n_{\text{prod}}=32\,700\,000$  for  $L=350$ . Since we took measurements only every  $n_{\text{flip}}=8$  sweeps, the number of total measurements per run is  $n_{\text{meas}}=n_{\text{prod}}/n_{\text{flip}}$ . We left at least  $20n_{\text{flip}}\tau_e$  thermalization sweeps before taking measurements.<sup>21-23</sup> To estimate the autocorrelation time of the energy measurements,  $\tau_e$ , we have applied two different methods. First, we use the fact that  $\tau_e$  enters the error estimate  $\epsilon_{\text{JK}} = \sqrt{2} \tau_e / n_{\text{meas}} \epsilon_{\text{naive}}$  for the mean energy  $\langle E \rangle$  of  $n_{\text{meas}}$  correlated energy measurements of variance

FIG. 2. Energy histograms for  $L=100$  and  $\beta_{MC}^{PBC}=1.342027$  and  $\beta_{MC}^{FBC}=1.3378$ .

$$\epsilon_{\text{naive}}^2 = \sum_{j=1}^{n_{\text{meas}}} (\langle E \rangle - E_j)^2 / (n_{\text{meas}} - 1).$$

The “true” error estimate  $\epsilon_{\text{JK}}$  is obtained splitting the energy time series into 50 bins, which were in their turn jackknived<sup>24,25</sup> to decrease the bias in the analysis. The second way of obtaining  $\tau_e$  is by a direct computation of the integrated autocorrelation time

$$\tau_e^{\text{int}} = \frac{1}{2} + \sum_{j=1}^{k_{\text{max}}-1} (1 - j/k_{\text{max}}) \times \frac{1}{k_{\text{max}} - (j-1)} \frac{\sum_{i=1}^{k_{\text{max}}-(j-1)} (E_i - \langle E \rangle)(E_{i+j} - \langle E \rangle)}{\langle E^2 \rangle - \langle E \rangle^2},$$

where  $k_{\text{max}}$  is a suitable cutoff<sup>21</sup> around  $6\tau_e^{\text{int}} < k_{\text{max}} < 10\tau_e^{\text{int}}$ . The corresponding error in  $\tau_e^{\text{int}}$  is derived from the *a priori* formula  $\sqrt{2} (2k_{\text{max}} + 1) / n_{\text{meas}} \tau_e^{\text{int}}$ .

In Fig. 1 we present the energy time series for the  $L=300$  and  $\beta_{MC}=1.34146$  simulation runs. The expected characteristic behavior for a first-order phase transition can be clearly seen. The system remains in one of the two coex-

TABLE III. Extrema for the (finite lattice) specific heat  $C_{\text{max}}$ , the susceptibility  $\chi_{\text{max}}$ , and the energetic Binder parameter  $B_{\text{min}}$  together with their respective pseudocritical inverse temperatures.

$L$	$\beta_{\text{max}}^C$	$C_{\text{max}}$	$\beta_{\text{max}}^\chi$	$\chi_{\text{max}}$	$\beta_{\text{min}}^B$	$B_{\text{min}}$
70	1.334469(53)	89.26(96)	1.334212(52)	95.3(1.2)	1.333966(52)	0.660221(74)
84	1.336360(46)	124.6(1.4)	1.336215(45)	143.8(1.7)	1.336040(46)	0.660441(71)
100	1.337705(34)	171.3(1.9)	1.337620(33)	210.5(2.5)	1.337492(33)	0.660657(69)
126	1.339124(33)	268.4(4.1)	1.339081(33)	355.8(5.7)	1.339000(33)	0.660774(94)
150	1.339905(25)	391.5(7.4)	1.339881(25)	550(11)	1.339821(25)	0.66058(12)
200	1.340747(23)	757(16)	1.340739(22)	1144(25)	1.340704(22)	0.66006(15)
226	1.341046(18)	1006(27)	1.341042(18)	1554(43)	1.341014(18)	0.65981(19)
250	1.341229(15)	1285(29)	1.341225(15)	2033(47)	1.341203(15)	0.65950(17)
278	1.341379(12)	1695(42)	1.341377(12)	2735(69)	1.341358(12)	0.65900(20)
300	1.341493(12)	2083(51)	1.341491(12)	3413(86)	1.341475(12)	0.65856(21)
350	1.3416496(92)	3176(77)	1.3416490(92)	5338(130)	1.3416373(92)	0.65754(23)

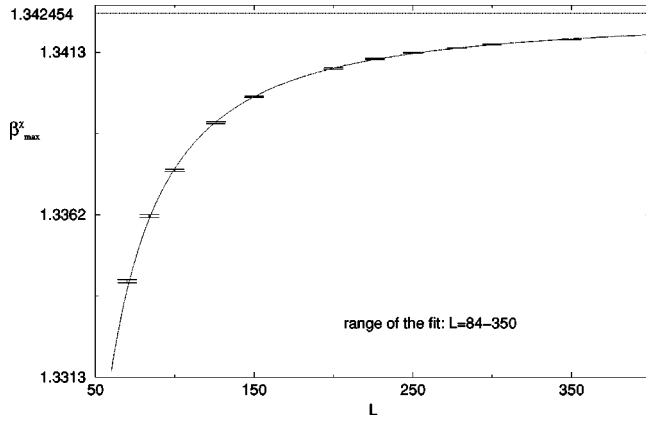


FIG. 3. Finite-size scaling analysis of the pseudocritical  $\beta_{\max}^X$  in the range  $L=84-350$  by means of the ansatz  $\beta_{\max}^X(L)=\beta_c+e_1/L+e_2/L^2$ . The infinite-volume critical point obtained from the fit is  $\beta_c=1.342478(38)$ , with a goodness of fit  $Q=0.13$ .

isting phases for a long period of time. The energy histogram for the full series is also presented in this figure. The similar height of the two peaks confirms that the simulation was performed very near the pseudocritical inverse temperature.

It is instructive to compare the energy histograms corresponding to the adoption of fixed or periodic boundary conditions. To this end we have performed two different Monte Carlo runs, close to the respective pseudocritical inverse temperatures, which are  $\beta_{MC}^{PBC}=1.342027$  and  $\beta_{MC}^{FBC}=1.3378$  for a lattice size  $L=100$ . These simulations have been done using 8 000 000 production sweeps, with  $n_{\text{flip}}=8$ , discarding the initial 250 000 (150 000) sweeps in the case of PBC's (FBC's) for the thermalization of the system. Both histograms can be seen in Fig. 2. They show the characteristic two-peak structure. Nevertheless, the latent heat, i.e., the separation between the maximum of the two peaks, is clearly smaller for fixed boundary conditions. This qualitative observation suggests that a simple analysis of the energy histograms of a true first-order phase transition simulated with fixed boundary conditions might be misleading. Effectively, if the lattice size is not large enough, the energy histogram could show (apparently) a single peak and, in consequence, one can get the erroneous conclusion that the model exhibits a second-order phase transition. Nevertheless, even with FBC's the evolution of the energy histograms when the size of the system increases shown in Fig. 2 ( $L=100$ ) and in Fig. 1 ( $L=300$ ) exhibits the expected behavior of a first-order transition. This observation may be relevant in the interpretation of the analysis of Baig and Fort,<sup>4</sup> where a disappearance of a two-peak structure was observed when FBC's were imposed on the system.<sup>26</sup>

In addition to the qualitative analysis of the histograms, we have computed the specific heat, magnetic susceptibility and the Binder kurtosis parameter at nearby values of  $\beta_{MC}$  by means of standard reweighting techniques.<sup>27</sup> They are defined as

$$C(\beta)=\frac{\beta^2}{L^2}(\langle E^2 \rangle - \langle E \rangle^2), \quad (4)$$

TABLE IV. Pseudocritical inverse temperature fits.  $Q$  is the goodness of fit. Recall that the exact critical inverse temperature for the model is  $\beta_c(\text{exact})=\ln[1+\sqrt{(8)}]=1.342454\dots$

Range L's	$\beta_{\max}^C(L)=\beta_c+a_1/L+a_2/L^2$			$\beta_{\max}^X(L)=\beta_c+a_1/L+a_2/L^2$			$\beta_{\max}^B(L)=\beta_c+a_1/L+a_2/L^2$		
	$Q$	$\beta_c$	$a_2$	$Q$	$\beta_c$	$a_2$	$Q$	$\beta_c$	$a_2$
84-350	0.11	1.342494(38)	-0.219(15)	0.13	1.342478(38)	-0.208(15)	0.13	1.342481(38)	-0.210(15)
100-350	0.72	1.342423(46)	-0.187(19)	0.73	1.342408(46)	-0.177(18)	0.73	1.342412(46)	-0.180(18)

TABLE V. Fits on the extrema of  $C_{\max}$ ,  $\chi_{\max}$ , and  $B_{\min}$ .

Range $L$ 's	$C_{\max}(L)=c_0+c_1L+c_2L^2$			$\chi_{\max}(L)=e_0+e_1L+e_2L^2$			$B_{\min}(L)=B_0+B_1/L+B_2/L^2$					
	$Q$	$c_0$	$c_1$	$c_2$	$Q$	$e_0$	$e_1$	$e_2$	$Q$	$B_0$	$B_1$	$B_2$
100–350	0.012	254(25)	-4.24(35)	0.0342(11)					0.011	0.65461(40)	1.52(13)	-92.1(9.2)
126–350	0.15	427(65)	-6.14(75)	0.0389(29)	0.033	766(101)	-11.9(1.2)	0.0691(31)	0.11	0.65295(72)	2.19(28)	-153(24)
150–350					0.38	1262(203)	-16.7(2.1)	0.0798(49)				

$$\chi(\beta) = \frac{\beta^2}{L^2} (\langle M^2 \rangle - \langle M \rangle^2), \quad (5)$$

$$B(\beta) = 1 - \frac{\langle E^4 \rangle}{3\langle E^2 \rangle^2}. \quad (6)$$

In Table III we show the extrema of the magnitudes defined above, together with their pseudocritical inverse temperatures. The error bars of these quantities have been estimated splitting the time-series data into 50 bins, which were jackknived to decrease the bias in the analysis of reweighted data.

#### IV. SCALING LAWS ANALYSIS

Once we have the results from the numerical simulation on finite lattices, we can proceed to analyze the data imposing the scaling laws of Table I.

##### A. Analysis of the pseudocritical inverse temperature

In Table IV we present the results of fitting the pseudocritical betas of  $C_{\max}$ ,  $\chi_{\max}$ , and  $B_{\min}$  to the ansatz  $\beta_c + a_1/L + a_2/L^2$  suggested by the finite-size scaling laws presented in Table I. Notice that we have performed two sets of fits: one for the full range  $84 \leq L \leq 350$  and a second including only results from the lattice sizes  $100 \leq L \leq 350$ . Notice that the fits are extremely good even for the initial range  $84 \leq L \leq 350$ , but they improve slightly if  $L = 84$  is discarded. Remember that reasonable fits should have a goodness of fit,<sup>28</sup>  $Q$  above 0.05. Figure 3 depicts the fit for  $\beta_{\chi}^{\max}(L)$  in the range  $84 \leq L \leq 350$ . The *exact* critical inverse temperature for the 2D eight-state Potts model is  $\beta_c(\text{exact}) = \ln[1 + \sqrt{8}] = 1.342454\dots$ . Our results of Table IV are in perfect agreement with this value.

We have also fitted our data to the ansatz  $\beta_c^{\text{peaks}} = \beta(\infty) + \theta_1/L^2 + \theta_2/L^4$  corresponding to the PBC finite-size scaling law. Even though the goodness of fit  $Q$  obtained does not allow one to discard the fits, the infinite volume  $\beta_c(\infty)$  resulting from them does not coincide with the exactly known value, showing that this ansatz is unsuitable. I.e., for the  $\beta_{\max}^C(L)$  in the range  $84 \leq L \leq 350$ , the fit produces  $Q = 0.10$  and  $\beta_c(\infty) = 1.342063(11)$  and for  $\beta_{\max}^X(L)$  in the range  $100 \leq L \leq 350$ , the results are  $Q = 0.21$  and  $\beta_c(\infty) = 1.342079(13)$ .

##### B. Analysis of $C_{\max}$ , $\chi_{\max}$ , and $B_{\min}$

The results of the fits to the specific heat and susceptibility maxima  $C_{\max}$  and  $\chi_{\max}$ , together with the kurtosis minimum, are summarized in Table V. As before, we show the fits for two ranges of lattice sizes. Notice that the linear correction coefficients  $c_1$  and  $e_1$  are two orders of magnitude larger than the coefficients  $c_2$  and  $e_2$  of the dominant contribution  $L^2$ . This makes it necessary to adjust the data to the ansatz  $C_{\max}(L) = c_0 + c_1L + c_2L^2$  and allows us to estimate the corrections to the leading term.

In simulations with PBC's, the correction to the leading term is of the order  $\gamma_1/L^2$ . If we fit our specific heat data in the range  $L = 126-350$  to the ansatz  $C_{\max}(L) = \gamma_0 + \gamma_1/L^2 + \gamma_2L^2$ , the goodness of fit is  $Q = 0.0003$  with an absurdly high value for  $\gamma_1$ . On the other hand, if we do not allow for a correction term and fit the data to  $C_{\max}(L) = \gamma_0 + \gamma_2L^2$ , the goodness of fit turns out to be 0.

The work of Medved<sup>7</sup> shows that the coefficient of  $L^2$  in the finite-size scaling of  $C_{\max}$  is related to the latent heat  $\Lambda_{\text{FBC}}$  via  $c_2 = (\Lambda_{\text{FBC}} \beta_c / 2)^2$ . In fact, it is the same relationship that holds for periodic boundary conditions.<sup>14,16,17</sup> If we use our estimation  $c_2 = 0.0389(29)$  from Table V and  $\beta_c = \ln[1 + \sqrt{8}]$ , we obtain for the latent heat

$$\Lambda_{\text{FBC}} = 0.294(11). \quad (7)$$

Another way of estimating the latent heat is from the direct calculation, right at the transition, of the internal energies per site of the ordered and disordered phases,  $e_{\text{ord}}$

TABLE VI. Finite-size estimates  $e_o(L)$  and  $e_d(L)$ . They are obtained by reweighting the energy histograms until both peaks have equal heights. The infinite-volume ordered and disordered energies are estimated from the ansatz  $e_o(L) = e_{\text{ord}} + k_1/L$  and  $e_d(L) = e_{\text{dis}} + k_2/L$ .

$L$	$e_o$	$e_d$
100	-1.580(11)	-1.4167(74)
126	-1.586(10)	-1.398(20)
150	-1.587(18)	-1.398(13)
226	-1.5965(93)	-1.3623(91)
250	-1.5944(83)	-1.362(14)
278	-1.5970(39)	-1.350(17)
300	-1.5960(27)	-1.3452(98)
350	-1.5958(31)	-1.337(13)
:	:	:
$\infty$	-1.6032(48)	-1.3114(92)

$=E_{\text{ord}}/V$  and  $e_{\text{dis}}=E_{\text{dis}}/V$ . Of course, the latent heat is just  $\Lambda=e_{\text{dis}}-e_{\text{ord}}$ . Lee and Kosterlitz proposed<sup>29</sup> to reweight a given energy histogram until both peaks have equal height. The locations of the two maxima in the histogram can be taken as finite-size estimates,  $e_o(L)$  and  $e_d(L)$ , for the infinite-volume limits at  $\beta_c$  of  $e_{\text{ord}}$  and  $e_{\text{dis}}$ . The scaling of  $e_o(L)$  and  $e_d(L)$  for fixed boundary conditions<sup>7</sup> as well as periodic boundary conditions<sup>29</sup> is  $e_o(L)=e_{\text{ord}}+O(1/L)$  and  $e_d(L)=e_{\text{dis}}+O(1/L)$ .

We smoothed<sup>28</sup> our energy histograms to reduce the noise and searched for  $e_o(L)$  and  $e_d(L)$ . Table VI shows the estimations that we found. Fitting them to the ansatz  $e_o(L)=e_{\text{ord}}+k_1/L$  and  $e_d(L)=e_{\text{dis}}+k_2/L$ , we obtained  $e_{\text{ord}}=-1.6032(48)$  and  $e_{\text{dis}}=-1.3114(92)$ , with goodness of fit<sup>28</sup>  $Q=1$  and  $Q=0.9$ , respectively. Consequently another estimation for the latent heat is

$$\Lambda=0.292(10). \quad (8)$$

The agreement with our previous estimation could not be better: it is quite comforting.

Baxter<sup>30,31</sup> derived an analytical expression for the latent heat of the  $q$ -state Potts model assuming periodic boundary conditions. Numerical evaluations of his expression are tabulated in Wu<sup>20</sup> and Janke.<sup>17</sup> For  $q=8$ , the latent heat for the Potts model with periodic boundary conditions is  $\Lambda_{\text{PBC}}=0.486358\dots$ . Obviously our estimations of the latent heat do not coincide with this value, but it should not be so surprising in view of Fig. 2, where it can be seen that, for  $L=100$ , the distance between peaks for PBC's is so different

from the distance between peaks for FBC's. Although such differences could tend towards the same value with  $L\rightarrow\infty$ , our analysis indicates that in fact they do not.

Notice that, unlike the latent heat, the analytically known infinite-volume critical inverse temperature  $\beta_c=\ln[1+\sqrt{(q)}]$  for the  $q$ -state Potts model is derived<sup>8,31-33</sup> using the self-duality property of the model, which is independent of boundary conditions when  $L\rightarrow\infty$ . Let us recall that our estimations of  $\beta_c$  are consistent with  $\beta_c=1.342454\dots$ .

## V. CONCLUSIONS

The first-order phase-transition finite-size scaling laws for fixed boundary condition lattices of Borgs, Kotecky, and Medved have been presented, tested, and shown to be the only ones that hold for the 2D eight-state Potts model.

It is clear from our analysis that Monte Carlo simulations for FBC's are necessarily going to be much more time consuming than those for PBC's, since for PBC's the system sets into the finite-size scaling region as  $\beta_c(L)=\beta_c(\infty)+\theta_1/L^d$ , while for FBC's it does it at the slower pace of  $\beta_c(L)=\beta_c(\infty)+a_1/L$ . Besides, we have found that the latent heat is affected by the boundaries.

## ACKNOWLEDGMENTS

It is a pleasure to thank W. Janke and A. Salas for very stimulating discussions. Financial support from CICYT Contracts Nos. AEN98-0431 and AEN99-0766 is acknowledged.

- 
- <sup>1</sup>K. Binder and D. W. Heermann, *Monte Carlo Simulation in Statistical Physics: An Introduction* (Springer, Berlin, 1988).
- <sup>2</sup>M. Baig, D. Espriu, D.A. Johnston, and R.P.K.C. Malmini, *J. Phys. A* **30**, 405 (1997).
- <sup>3</sup>M. Baig, D. Espriu, D.A. Johnston, and R.P.K.C. Malmini, *J. Phys. A* **30**, 7695 (1997).
- <sup>4</sup>M. Baig and H. Fort, *Phys. Lett. B* **332**, 428 (1994).
- <sup>5</sup>C. Borgs and R. Kotecký, *J. Stat. Phys.* **61**, 79 (1990).
- <sup>6</sup>C. Borgs and R. Kotecký, *J. Stat. Phys.* **79**, 43 (1995).
- <sup>7</sup>I. Medved, Diploma thesis, Charles University, Prague, 1996.
- <sup>8</sup>R.B. Potts, *Proc. Cambridge Philos. Soc.* **48**, 106 (1952).
- <sup>9</sup>G.K. Saviddy and F.J. Wegner, *Nucl. Phys. B* **413**, 605 (1994).
- <sup>10</sup>J. Clua, Ph.D. thesis, Universitat Autònoma de Barcelona, 1998; M. Baig, J. Clua, D.A. Johnston, and R. Villanova (unpublished).
- <sup>11</sup>J. Jersak, C.B. Lang, and T. Neuhaus, *Phys. Rev. D* **54**, 6909 (1996).
- <sup>12</sup>V. Privman and M.E. Fisher, *J. Stat. Phys.* **33**, 285 (1983).
- <sup>13</sup>K. Binder and D.P. Landau, *Phys. Rev. B* **30**, 1477 (1984).
- <sup>14</sup>M.S.S. Challa, D.P. Landau, and K. Binder, *Phys. Rev. B* **34**, 1841 (1986).
- <sup>15</sup>C. Borgs and R. Kotecký, *Phys. Rev. Lett.* **68**, 1734 (1992).
- <sup>16</sup>C. Borgs, R. Kotecký and S. Miracle-Solé, *J. Stat. Phys.* **62**, 529 (1991).
- <sup>17</sup>W. Janke, *Phys. Rev. B* **47**, 14 757 (1993).
- <sup>18</sup>K. Binder, *Annu. Rev. Phys. Chem.* **43**, 33 (1992).
- <sup>19</sup>B.V. Enüstün, H.S. Sentürk, and O. Yurdakel, *J. Colloid Interface Sci.* **65**, 509 (1978); S.C. Mraw and D.F. Naas-O'Rourke, *Science* **205**, 901 (1979); J.F. Wendelken and C.-C. Wang, *Phys. Rev. B* **32**, 7542 (1985); V.N. Bogometav, E.V. Kolla, and Yu Kumzerov, *JETP Lett.* **41**, 34 (1985); R. Marx, *Phys. Rep.* **125**, 1 (1985); B.A. Weinstein, *Semicond. Sci. Technol.* **4**, 283 (1989); B. Gorbunov, L.S. Lazareva, A.Z. Gogolev, and E.L. Zhuzhgov, *Kolloidn. Zh.* **51**, 921 (1990).
- <sup>20</sup>F.Y. Wu, *Rev. Mod. Phys.* **54**, 235 (1982).
- <sup>21</sup>A. D. Sokal (unpublished).
- <sup>22</sup>N. Madras and A.D. Sokal, *J. Stat. Phys.* **50**, 109 (1988).
- <sup>23</sup>W. Janke, in *Computational Physics: Selected Methods—Simple Exercises—Serious Applications*, edited by K. H. Hoffmann and M. Schreiber (Springer, Berlin, 1996), p. 10.
- <sup>24</sup>R.G. Miller, *Biometrika* **61**, 1 (1974).
- <sup>25</sup>B. Efron, *The Jackknife, the Bootstrap and other Resampling Plans* (SIAM, Philadelphia, PA, 1982).
- <sup>26</sup>If this is the case, the phase transition of the 4D U(1) gauge model with FBC's will remain of first order. This point is still under study [M. Baig and R. Villanova (unpublished)].
- <sup>27</sup>A.M. Ferrenberg and R.H. Swendsen, *Phys. Rev. Lett.* **61**, 2635 (1988).
- <sup>28</sup>W. H. Press, B. P. Flannery, S. A. Teukolsky, and W. T. Vetterling, *Numerical Recipes—The Art of Scientific Computing* (Cam-

- bridge University Press, Cambridge, England, 1986).
- <sup>29</sup>J. Lee and J.M. Kosterlitz, Phys. Rev. Lett. **65**, 137 (1990); Phys. Rev. B **43**, 3265 (1991).
- <sup>30</sup>R.J. Baxter, J. Phys. C **6**, L445 (1973); using results from his article in J. Stat. Phys. **9**, 145 (1973).
- <sup>31</sup>R. J. Baxter, *Exactly Solved Models in Statistical Mechanics* (Academic Press, London, 1982).
- <sup>32</sup>F.Y. Wu and Y.K. Wang, J. Math. Phys. **17**, 439 (1976).
- <sup>33</sup>A. Hintermann, H. Kunz, and F.Y. Wu, J. Stat. Phys. **19**, 623 (1978).